Heliyon 10 (2024) e34962

Contents lists available at ScienceDirect

Heliyon

journal homepage: www.cell.com/heliyon

Research article

Facile synthesis of copper carbonate analog with peroxidase-like activity for colorimetric detection of isoniazid

Yan Dai [a], Hao Zhang [b,*]

[a] Chongqing Orthopedic Hospital of Traditional Chinese Medicine, Chongqing, 400012, China
[b] Chongqing Engineering Research Center of Pharmaceutical Sciences, Chongqing Medical and Pharmaceutical College, Chongqing, 401331, China

ARTICLE INFO

Keywords:
Copper carbonate analog
Peroxidase-like activity
Nanozyme
Colorimetric detection
Isoniazid

ABSTRACT

In this article, copper carbonate analog with good peroxidase-like activity was successfully synthesized for the first time *via* a simple co-precipitation of $CuSO_4$▪$5H_2O$ and Na_2CO_3. The obtained copper carbonate analog exhibited excellent intrinsic peroxidase-like activity towards a classical peroxidase substrate of 3, 3′, 5, 5′ -tetramethylbenzidine (TMB) in the presence of hydrogen peroxide (H_2O_2) under an acidic environment. The study of the catalytic mechanism confirmed that the hydroxyl radical produced from the decomposition of H_2O_2 is the main reactive oxygen species responsible for the catalytic oxidation of TMB to oxTMB. Moreover, results from kinetic parameter analysis indicated that H_2O_2 was more easily and/or likely to attach to the copper carbonate analog than TMB. Subsequently, the effects of experimental conditions (buffer pH, temperature, and incubation time) on the catalytic activity of the copper carbonate analog were also optimized. Finally, a copper carbonate analog-based colorimetric sensor was developed to determine isoniazid. Under the optimal conditions, the linear range for isoniazid was as broad as 0–178.6 μM, and the detection limit was as low as 8.47 μM. The spiked recoveries of isoniazid in normal human serum has been observed in the range of 94.8%–105.5 %. This strategy focuses on the development of a green, cost-efficient peroxidase mimic with high activity, good biocompatibility, and a simple synthesis process.

1. Introduction

Horseradish peroxidase (HRP, EC 1.11.1.7) is an important catalyst in living organisms and can effectively catalyze many biochemical reactions [1]. Owing to its remarkable efficiency, versatility, and specificity for substrates, HRP has been found to be of great importance in catalytic and diagnostic processes [2–4]. In analytical diagnostics, HRP is able to generate distinctive colors when it interacts with hydrogen peroxide (H_2O_2) and various substrates, such as 3,3′,5,5′-tetramethylbenzidine (TMB), *o*-phenylenediamine, and diaminobenzidine [5,6]. Nevertheless, the application of peroxidase always suffers from certain limitations such as low stability, lack of reusability, high cost, and sensitivity to the surrounding environment (strong acidic and basic or high temperature) [7–9]. Taking advantage of the remarkable progress in nanotechnology, nanozymes have been viewed as a viable substitute for natural enzymes, as they possess high stability, design flexibility, cost-effectiveness, robustness, and tunable catalytic activity [10–13].

So far, lots of nanomaterials, such as iron single-atom catalysts [14], carboxymethylcellulose-platinum nanoparticles [15], and

* Corresponding author. Chongqing Engineering Research Center of Pharmaceutical Sciences, Chongqing Medical and Pharmaceutical College, Chongqing 401331, China.
E-mail address: 2110011@cqmpc.edu.cn (H. Zhang).

https://doi.org/10.1016/j.heliyon.2024.e34962
Received 30 July 2023; Received in revised form 1 June 2024; Accepted 19 July 2024
Available online 20 July 2024

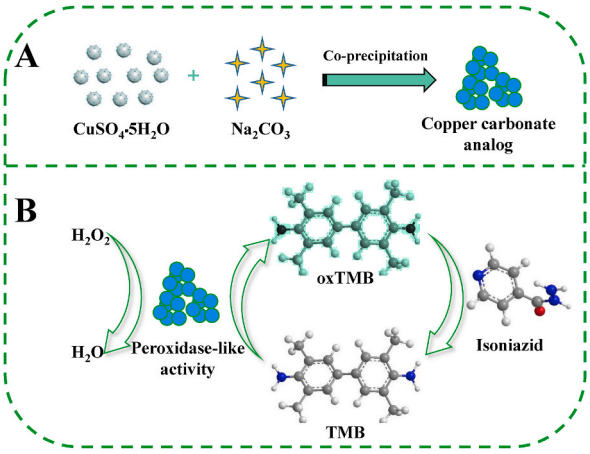

Fig. 1. Schematic illustration of the synthesis process of copper carbonate analog (**A**) and its application in colorimetric sensing of isoniazid (**B**).

Fe–N/C single-atom nanozyme [16], have been demonstrated to serve as enzyme mimics similar to natural enzymes such as peroxidase [14], laccase [15] or oxidase [16]. These nanomaterials have been widely used in clinical diagnosis, nanomedicine, and environmental monitoring. For example, nanomaterials with oxidase-like catalytic activity can catalyze the corresponding enzymatic substrates to produce color changes, which has been utilized to construct colorimetric biosensors. Shen et al. [17] developed a colorimetric method to detect organophosphorus pesticides by directly oxidizing the chromogenic substrate of *o*-phenylenediamine to 2,3-diaminophenothiazine. Moreover, the biomedical applications of nanozymes have also been reported, including bacterial infections, relief of tumor hypoxia, and inhibition of metastasis. Zhang et al. developed a CuS@Pt–Au/aptamer nanozyme for the synergistic therapy of wound infections in diabetic mice. The nanozyme exhibits the release of hydroxyl radicals and excellent photothermal properties [18]. Many metal complexes are traditionally prepared under harsh conditions, such as high temperature and pressure, calcination, and reflux. These conditions not only pose challenges in terms of experimental difficulty and the need for specialized equipment, but they also increase the risks involved [19]. Moreover, it is unfavorable for large-scale preparation and application. Thus, exploring a green and cost-efficient peroxidase mimic with high activity, environmental friendliness, large-scale preparation, and a simple synthesis process is still of significance.

Currently, metallic oxides and salts, which are a large family of inorganic materials, have been widely used in analytical diagnostics, catalysis, and enzyme immobilization due to their chemical stability, good biocompatibility, and low cost [20–22]. For example, a phytic-acid modified $Cu_3(PO_4)_2·3H_2O$ organic-inorganic hybrid material with intrinsic peroxidase-like catalytic activity has been prepared by us [20]. Finally, the developed colorimetric method for hydrogen peroxide detection has a linear range of 0.1–5.0 mM and a detection limit of 0.079 mM. A laccase mimic enzyme based on copper ion and adenosine monophosphate has been prepared by Huang et al. [21] for the removal and detection of phenolic compounds. The linear range for phenolic compounds detection by nanozyme was 0.1–100 μM with a detection limit of 0.033 μM. Metal phosphate compound has been customarily used as support for enzyme immobilization. For example, a $Cu_3(PO_4)_2$-based hybrid nanoflower was successfully prepared for the immobilization of β-galactosidase [22]. The immobilized β-galactosidase possesses superior catalytic activity and stability, as well as long-term storage stability and reusability. As a member of metallic salt compounds, copper carbonate analog has been applied in fungal biomineralization [23] and supercapacitor [24]. Although the application of copper carbonate analog has been investigated, there remain several unknowns and challenges regarding its intrinsic catalytic activity as a peroxidase mimic.

Isoniazid, a synthetic antimicrobial, is one of the first-line drugs for the treatment of tuberculosis. However, irrational dosages not only have the potential to develop drug resistance and neurotoxicity, but may also be ineffective against tuberculosis. To ensure the effectiveness and safety of the drug, it is essential to analyze the level of isoniazid in the serum sample. Currently, various methods for isoniazid detection have been widely reported, such as high-performance liquid chromatography [25], fluorescence spectrophotometry [26], and electrochemical methods [27]. Despite the numerous advantages of these assays, they are generally expensive and time-consuming, requiring specialized testing equipment, technicians, and laborious sample preparation. For this reason, the colorimetric method has attracted widespread attention due to its advantages of a fast response, easy operation, and an obvious signal. Therefore, it is of great significance to establish a simple, rapid, and accurate isoniazid detection method based on the colorimetric method.

In this study, copper carbonate analog with excellent peroxidase-like activity was synthesized through a straightforward co-precipitation of $CuSO_4$▪$5H_2O$ and Na_2CO_3 (Fig. 1). The peroxidase-like activity of copper carbonate analog was demonstrated by catalyzing the reaction between H_2O_2 and TMB in an acidic environment. The catalytic mechanism of the copper carbonate analog has been systematically studied. The effects of experimental conditions (pH, temperature, and incubation time) on the catalytic activity of the copper carbonate analog and the kinetic parameters of the copper carbonate analog were systematically investigated, respectively. The aims of this work are: 1) Preparing a green and cost-efficient peroxidase mimic (copper carbonate analog) with high activity, good biocompatibility, and environmental friendliness; 2) Exploring the intrinsic catalytic activity of the copper carbonate analog as a

peroxidase mimic; 3) Establishing a simple, rapid, and accurate isoniazid detection method based on the colorimetric method; 4) Verifying the applicability of the developed strategy by detecting isoniazid in human serum.

2. Materials and methods

2.1. Chemicals and materials

L (+)-Glutamic acid was purchased from Shanghai Aladdin Biochemical Technology Co., Ltd. (Shanghai, China). Sodium hydroxide, isopropanol (IPA), and sodium chloride were purchased from Chengdu Jinshan Chemical Test Co., Ltd. (Chengdu, China). L-Serine was purchased from Tianjin Guangfu Fine Chemical Research Institute (General Partnership) (Tianjin, China). Copper (II) sulfate pentahydrate was purchased from Shanghai Macklin Biochemical Co., Ltd. (Shanghai, China). Superoxide dismutase (SOD), α-amylase, and trypsin were purchased from Shanghai Yuanye Bio-Technology Co., Ltd. (Shanghai, China). Ethanol absolute was purchased from Chongqing Chuandong Chemical (Group) Co., Ltd. (Chongqing, China). Sodium carbonate (Na_2CO_3), isoniazid, sodium bromide, TMB, and bovine albumin were obtained from Shanghai Adamas Reagent Co., Ltd. (Shanghai, China). Normal human serum was purchased from Beijing Solarbio Science and Technology Co., Ltd. (Beijing, China). L (+)-Sodium acetate anhydrous, acetic acid glacial, and hydrogen peroxide (30 %) were purchased from Chengdu Chron Chemicals Co., Ltd. (Chengdu, China).

2.2. Apparatus

Ultraviolet–visible (UV–vis) spectra were obtained by a UV-2600 spectrophotometer (Shimadzu Instruments (Suzhou) Co., Ltd.). A FE 28 pH meter was purchased from Mettler Toledo Technology (China) Co., Ltd. For measuring the pH of the solution. DHG-9035A drying oven was purchased from Shanghai Yiheng Technology Instrument Co., Ltd. ((Shanghai, China). UC-2H ultrasonic cleaner was purchased from Shanghai Titan Scientific Co., Ltd. (Shanghai, China). The surface property of the material was investigated by a SU8100 Scanning Electronic Microscopy (Hitachi, Japan). Transmission electron microscopy (TEM) images were collected with a JEM-2100F (JEOL, Japan). Infrared spectra was collected using a Nicolet iS50 FT-IR spectrophotometer (Thermo Fisher Scientific Inc.). The crystal structure of the material was studied by X'Pert Powder X-ray diffraction (XRD) (Empyrean, PANalytical, the Netherlands). X-ray photoelectron spectroscopy (XPS) was recorded employing a Escalab 250Xi (Thermo Fisher Scientific Inc.).

2.3. Study of the peroxidase-like activity of copper carbonate analog

The peroxidase-like activity of copper carbonate analog was investigated by recording the absorption spectra of oxidized TMB (oxTMB). To prepare the copper carbonate analog, 50.0 μL of $CuSO_4{\cdot}5H_2O$ (80.0 mM) solution was added into 50.0 μL of Na_2CO_3 (100.0 mM) solution. This resulted in the rapid precipitation of the copper carbonate analog, which was obtained by centrifugation for 1.0 min at 500 rpm. Then, the peroxidase-like activity of the copper carbonate analog was performed in the presence of 100 μL of sodium acetate buffer (10.0 mM, pH 4.0), 50 μL of absolute ethanol, 50 μL of H_2O_2 solution (0.24 mM) and 10 μL of TMB solution (0.099 mM) with a total reaction volume of 210.0 μL. After being reacted at 40 °C for 5.0 min, the reaction supernatant was obtained by centrifuging the reaction mixture at 500 rpm for 1.0 min. Next, 60.0 μL of the reaction supernatant (a uniform solution) was added to the microcuvette. Finally, the absorbance spectrum of the supernatant was recorded in the range of 500–750 nm using a UV-2600 spectrophotometer.

2.4. Catalytic mechanism of copper carbonate analog as peroxidase-like mimic

To explore the catalytic mechanism of copper carbonate analog as a peroxidase-like mimic, IPA and SOD radical scavengers were introduced to scavenge the reactive oxygen species of •OH and $O_2\bullet^-$, respectively. In brief, a total volume of 210.0 μL of reaction mixture containing 100 μL of sodium acetate buffer (10.0 mM, pH 4.0), 50 μL of H_2O_2 solution (0.24 mM), 10 μL of TMB solution (0.198 mM), and 50.0 μL of varied amounts of radical scavengers were incubated at 40 °C for 5.0 min, respectively. Next, 60.0 μL of the reaction supernatant (a uniform solution) was added to the microcuvette. Finally, the absorbance values at 652 nm were recorded.

2.5. Detection of the kinetic parameters of copper carbonate analog

The kinetic parameters of the copper carbonate analog were measured in the presence of 50.0 μL of $CuSO_4{\cdot}5H_2O$ (80.0 mM) solution, 50.0 μL of Na_2CO_3 (100.0 mM) solution, and 50 μL of absolute ethanol with various concentrations of TMB or H_2O_2. Next, 60.0 μL of the reaction supernatant (a uniform solution) was added to the microcuvette. The absorbance spectra of the reaction supernatant was recorded at 652 nm. The kinetic parameters were obtained according to the Michaelis-Menten equation [20].

2.6. Determination of isoniazid using the colorimetric method

Firstly, 100 μL of solution containing $CuSO_4{\cdot}5H_2O$ (19.05 mM) and Na_2CO_3 (23.81 mM) was mixed with 50 μL of different concentrations of isoniazid solution, and then incubated at 40 °C for 2.0 min. Subsequently, 50 μL of H_2O_2 (0.24 mM) and 10.0 μL of TMB solution (0.099 mM) were added to the above reaction mixture and incubated at 40 °C for 5.0 min. The reaction supernatant was obtained by centrifuging the reaction mixture at 500 rpm for 1.0 min. Next, 60.0 μL of the reaction supernatant (a uniform solution)

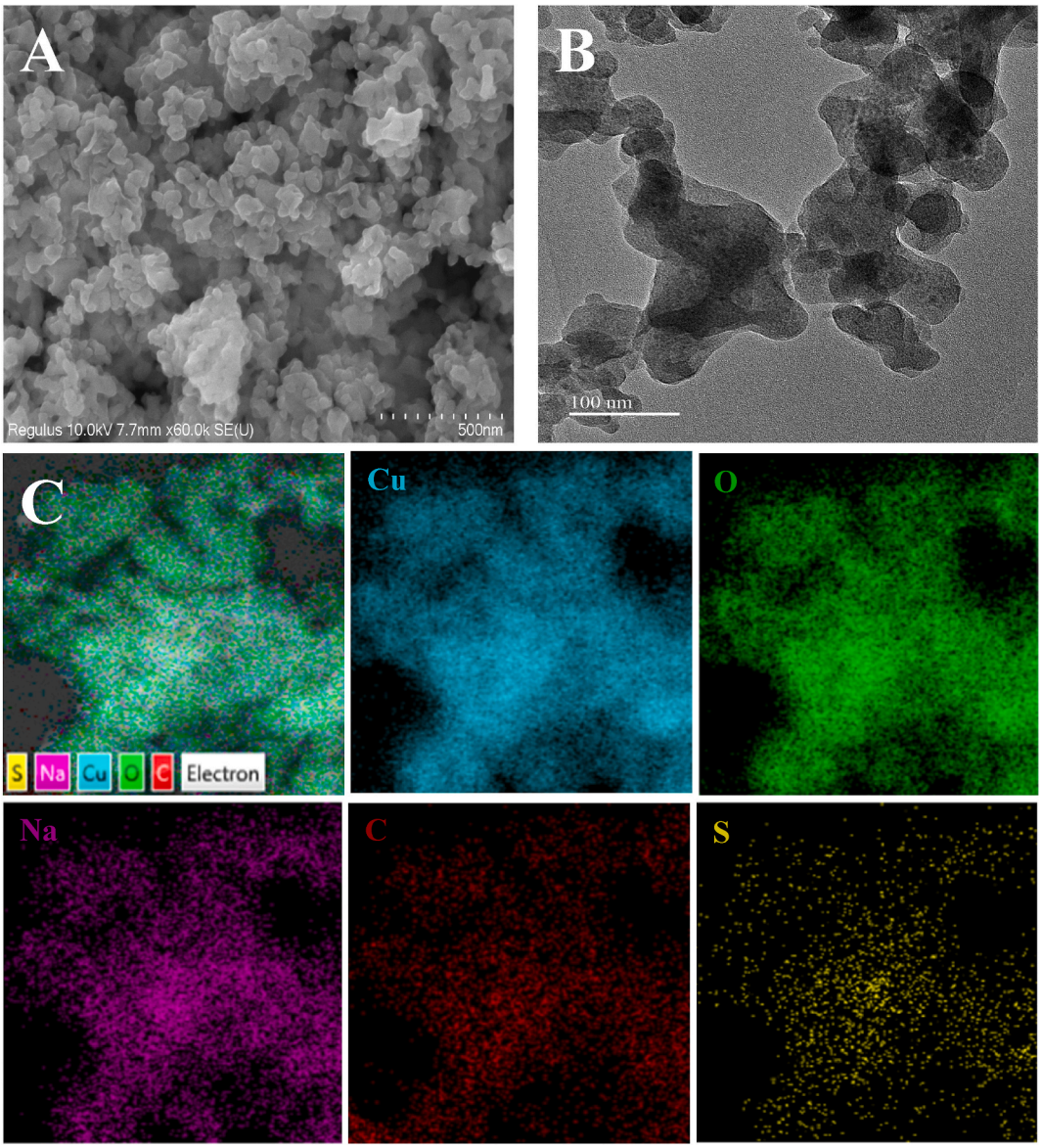

Fig. 2. (**A**) SEM and TEM (**B**) images of the synthesized copper carbonate analog; (**C**) EDS elemental mapping images of the synthesized copper carbonate analog.

was added to the microcuvette. Finally, the absorbance spectrum of the supernatant was taken at 652 nm using a UV-2600 spectrophotometer. A calibration curve between isoniazid concentrations and absorbance values was plotted. The reaction mixture solutions without the addition of isoniazid were used as the control group. The experiments were repeated at least three times.

2.7. Selectivity study

The selectivity of the colorimetric method for the detection of isoniazid was studied. The following possible interfering substances in serum samples were analyzed under optimal conditions: Cl^-, Na^+, urea, α-amylase, L-glutamic acid, L-serine, trypsin, and bovine albumin. The final concentrations of isoniazid and interfering substances were 0.016 mg/mL and 0.119 mg/mL, respectively.

3. Results and discussion

3.1. The characterizations of copper carbonate analog

The copper carbonate analog was prepared through a facile assembly procedure of Cu(II) and Na_2CO_3 in water (Fig. 1). The

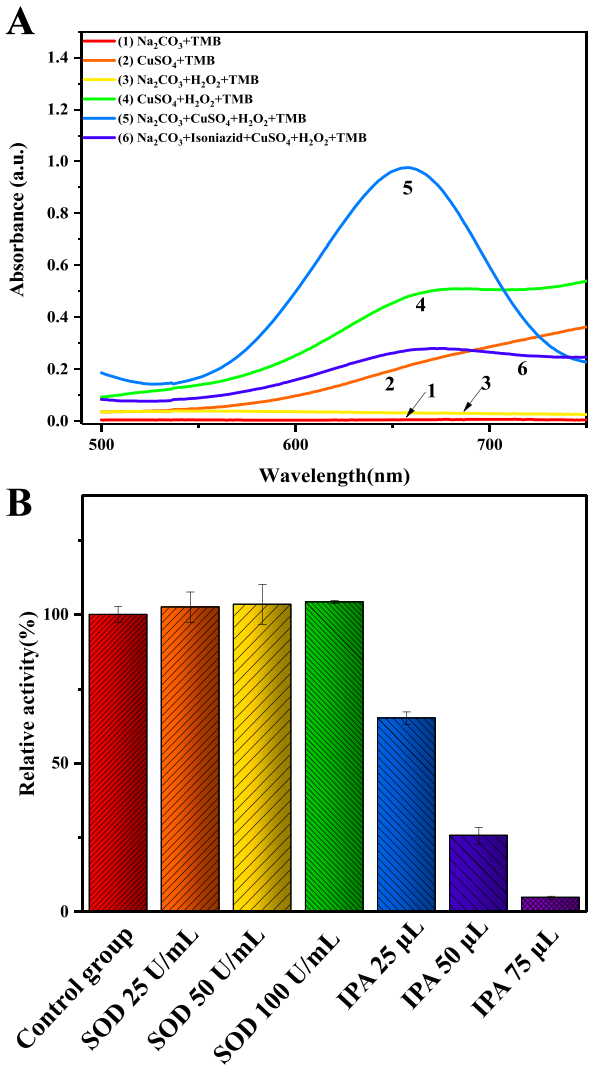

Fig. 3. (**A**) UV–Vis absorption spectra and digital photographs of (1) Na_2CO_3+TMB mixture solution, (2) $CuSO_4$+TMB mixture solution, (3) Na_2CO_3+TMB + H_2O_2 mixture solution, (4) $CuSO_4$+TMB + H_2O_2 mixture solution, (5) $CuSO_4$+Na_2CO_3+TMB + H_2O_2 mixture solution, (6) $CuSO_4$+Na_2CO_3+TMB + H_2O_2+ isoniazid mixture solution; (**B**) The effects of different radical scavengers of isopropanol and superoxide dismutase on the relative activity (%) of the synthesized copper carbonate analog. Error bars represent standard deviations ($n = 3$).

morphology of the copper carbonate analog was characterized by scanning electron microscopy (Fig. 2A). It can be seen that the copper carbonate analog presented an ellipsoidal shape nanostructure, indicating the successful synthesis of the copper carbonate analog. TEM images show that the copper carbonate analog has an ellipsoidal shape with a crystal lattice (Fig. 2B and Fig. S1). Moreover, EDX elemental mapping was employed to further analyze the surface characteristics of the copper carbonate analog, and the results showed that the elements Cu, O, Na, C, and S were distributed uniformly on the surface of the copper carbonate analog (Fig. 2C), thus confirming the presence of $CuSO_4$ and Na_2CO_3. XPS analysis was conducted to further examine the elemental composition of the copper carbonate analog (Fig. S2 and Table S1). The signals of Cu 2p, O 1s, C 1s, Na 1s, and S 2p can be observed in the XPS survey spectra (Fig. S2), which is in agreement with the EDX elemental mapping images. The contents of Cu, O, C, Na, and S are 18.29 %, 46.79 %, 31.51 %, 1.77 %, and 1.65 %, respectively. XRD measurements were employed to further investigate the physical phase and crystalline morphology of the copper carbonate analog. As shown in Fig. S3A, the XRD patterns of the copper carbonate analog display six main characteristic diffraction peaks, which are in agreement with the standard diffraction pattern of chalconatronite ($CuNa_2(CO_3)_2(H_2O)_3$) (JCPDS No. 71–1491). This confirms the successful synthesis of the copper carbonate analog with a crystal structure. To investigate the chemical bonding structure in copper carbonate analog, infrared spectra was collected as shown in Fig. S3B. The characteristic peak at approximately 3252 cm^{-1} was identified as the –OH stretching vibration of water molecules in the inter-layer, accompanied by the bending vibration of H–*O*–H at 1644 cm^{-1}, suggesting the existence of absorbed water molecules in the copper carbonate analog. The peaks at around 1456 cm^{-1}, 1355 cm^{-1}, and 1089 cm^{-1} were identified as the stretching vibrations of νOCO_2, and the asymmetrical and symmetrical stretching vibration modes of CO_3^{2-}, respectively [24,28].

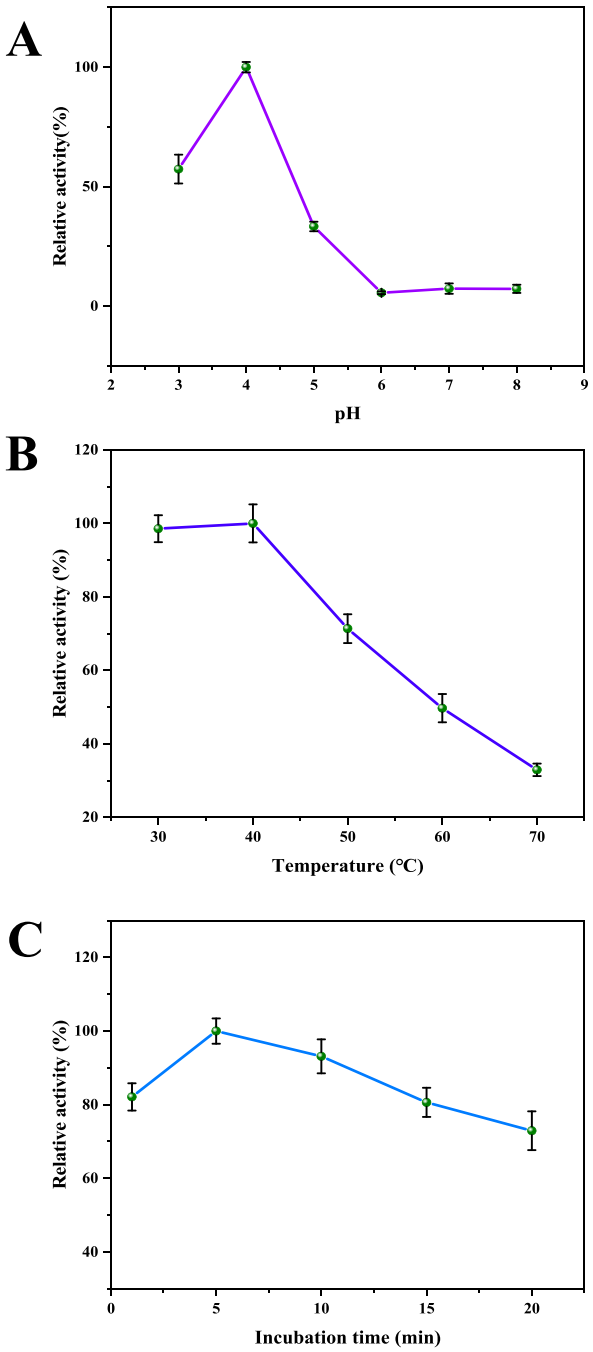

Fig. 4. The effects of buffer pH, temperature, and incubation time on the relative activity (%) of the synthesized copper carbonate analog. Error bars represent standard deviations ($n = 3$).

3.2. The peroxidase-like activity of copper carbonate analog

The peroxidase-like activity of copper carbonate analog was studied using TMB and H_2O_2 colorimetry. As shown in Fig. 3A, there are no obvious absorption peak observed for the Na_2CO_3+TMB solution (Figs. 3A and 1 curve) and the Na_2CO_3+TMB + H_2O_2 solution (Fig. 3A, 3 curve). A weak absorption peak can be observed for the $CuSO_4$+TMB solution (Figs. 3A and 2 curve) and the $CuSO_4$+TMB + H_2O_2 solution (Figs. 3A and 4 curve). However, a characteristic absorption peak of the chromogenic system at 652 nm was observed in the presence of $CuSO_4$, Na_2CO_3, TMB, and H_2O_2 (Figs. 3A and 5 curve). The results demonstrate that the exhibited peroxidase-like activity is derived from the as-synthesized copper carbonate analog, not from the $CuSO_4$ or Na_2CO_3 solution. Subsequently, the

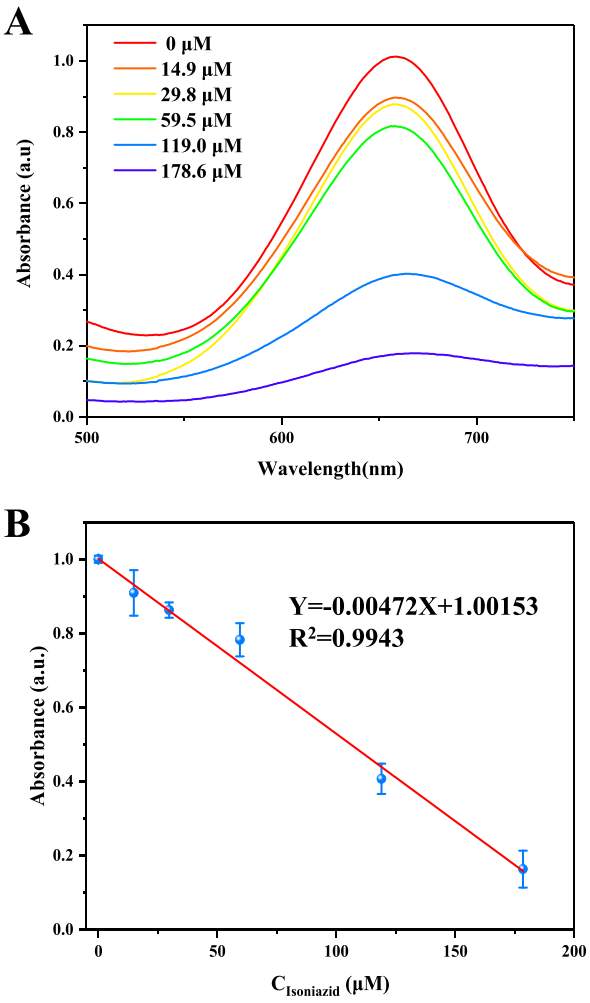

Fig. 5. UV–Vis absorption spectra corresponding to different concentrations of isoniazid (**A**); The corresponding calibration plots of isoniazid (**B**). Error bars represent standard deviations ($n = 3$).

characteristic absorption peak of the chromogenic system at 652 nm is used as a readout signal to evaluate the peroxidase-like activity. Finally, a weak absorption peak at 652 nm can be observed after the addition of isoniazid to the $CuSO_4$+Na_2CO_3+TMB + H_2O_2 solution (Figs. 3A and 6 curve). The results demonstrate that the developed method can be used to detect isoniazid.

3.3. Catalytic mechanism

To gain a better understanding of the catalytic mechanism of copper carbonate analog towards TMB and H_2O_2, different quenching agents were utilized to scavenge the reactive oxygen species (•OH or O_2•$^-$) that participate in the catalytic process. SOD and IPA are generally employed to scavenge the reactive oxygen species of O_2•$^-$ and •OH, respectively. As shown in Fig. 3B, the relative activity (%) remains almost unchanged after the introduction of SOD with different concentrations to the copper carbonate analog-TMB-H_2O_2 system. However, with the addition of IPA to the copper carbonate analog-TMB-H_2O_2 system, the relative activity (%) significantly decreased with the increasing amount of IPA. These results indicate that the hydroxyl radical (•OH) produced from the decomposition of H_2O_2 is the primary reactive oxygen species responsible for catalyzing the oxidation of TMB to oxTMB.

3.4. Optimization of the reaction conditions

Similar to HRP, the peroxidase-like activity of copper carbonate analog can be influenced by pH and temperature. Thus, the effects of buffer pH and temperature on the peroxidase-like activity of the copper carbonate analog were explored. As shown in Fig. 4A, the relative activity (%) of the copper carbonate analog increased first and then decreased significantly with the buffer pH increasing from 4.0 to 6.0. The catalytic activity remained almost constant in the pH range of 6.0–8.0, which may be due to the fact that the formation of the reactive intermediate (•OH) is more favorable in an acidic environment than in a basic one [29]. As shown in Fig. 4B, the relative

Table 1
Comparison with the performance of other analytical techniques for isoniazid detection.

Nanomaterial	Synthesis time	Detection methods	Linear range (μM)	LOD (μM)	Ref.
CuO/NiO	> 24 h	Colorimetry	1–20	0.4	[30]
Cr decorated *N*-doped carbon	> 34 h	Colorimetry	0.25–50	0.22	[31]
MXene $Ti_3C_2T_x$	> 24 h	Voltammetry	100–4600	64	[27]
Carbon quantum dots	5 h	Fluorimetry	3.81–210	1.14	[32]
β-cyclodextrin doped carbon dots	12 h	Fluorimetry	1.46–364.59	1.02	[33]
Cu–Fe Prussian blue analog nanocube	> 48 h	Colorimetry	1–100	0.44	[34]
Heparin sodium stabilized platinum nanoparticles	2 h	Colorimetry	2.5–250	1.7	[35]
Rhodium	/	Voltammetry	70–1300	13	[36]
Carbon dots	1.5 h	Fluorimetry	4–140	1.15	[37]
Tungsten disulfide/carbon nanotubes	16.5 h	Electrochemistry	10–80	0.24	[38]
Mo_2C/bimetallic zeolitic imidazolate framework	> 21 h	Electrochemistry	10–3500	1.5	[39]
Metal-organic framework-derived NiO@ZnO	> 9 h	Electrochemistry	0.8–800	0.25	[40]
Copper carbonate analog	1.0 min	Colorimetry	0–178.6	8.47	This study

activity (%) of the copper carbonate analog increased first and then decreased significantly with temperature increasing from 40 to 70 °C. However, the highest activity of the copper carbonate analog was observed at 40 °C. Moreover, the incubation time was also further explored. As shown in Fig. 4C, the highest activity of the copper carbonate analog was observed at 5.0 min. Therefore, the optimal reaction conditions were as follows: the buffer pH of 4.0, the temperature of 40 °C, and the incubation time of 5.0 min.

3.5. Kinetic parameter analysis

The peroxidase-like activity of copper carbonate analog was investigated by using TMB and H_2O_2 colorimetry. The kinetic parameters (K_m) were measured by catalyzing different concentrations of TMB or H_2O_2 in the presence of the copper carbonate analog as the catalyst. For H_2O_2 as a substrate, the Lineweaver-Burk double reciprocal plot displays a good linear correlation ($Y = 0.0316X+0.8177$, $R^2 = 0.9812$). The K_m value of the substrate (H_2O_2) is calculated to be 0.038 mM (Fig. S4 A and B). For TMB as a substrate, the Lineweaver-Burk double reciprocal plot displays a good linear correlation ($Y = 0.1026X+0.043$, $R^2 = 0.9993$), and the K_m value is calculated to be 2.39 mM (Fig. S4 C and D). The K_m value can approximate the magnitude of the affinity of the enzyme to the substrate. In general, a smaller K_m represents a stronger affinity of the enzyme to the substrate. Compared with previously reported HRP and other nanozymes (Table S2), the K_m value of the copper carbonate analog (2.39 mM) against TMB was higher than that of HRP and some other peroxidase-like nanozymes. However, the K_m of the copper carbonate analog against H_2O_2 (0.038 mM) is much lower than that of HRP and some other peroxidase-like nanozymes. Thus, it can be concluded that H_2O_2 is more easily and/or likely to attach to the copper carbonate analog than TMB due to the difference in the size of TMB and H_2O_2 molecules.

3.6. Colorimetric detection of isoniazid

Due to the presence of a hydrazide group, isoniazid can be used as a reducing agent to inhibit TMB oxidation [30,31]. Based on this, a colorimetric platform for the determination of isoniazid was developed. Fig. 5A shows the UV–visible absorption spectra with a decrease in the absorbance values of oxTMB at 652 nm as the concentrations of isoniazid increase from 0 to 178.6 μM. A good linear relationship was established between the absorbance value and the concentration of isoniazid. As shown in Fig. 5B, the linear calibration equation is $A = -0.00472X+1.00153$ (Where A is the absorbance value at 652 nm, X is the isoniazid concentrations, $R^2 = 0.9943$), and the linear range is from 0 to 178.6 μM. The detection limit of isoniazid is calculated to be 8.47 μM ($LOD = 3\sigma/S$, where S represents the slope of the calibration curve in Fig. 5B and σ is the standard deviation of eleven blank assays). Additionally, for nine batches of as-prepared copper carbonate analog, the relative standard deviation of absorbance values at 652 nm was 3.1 %. Table 1 presents a comparison of analytical techniques used to detect isoniazid with those of other reported methods. The colorimetric method proposed in this study has a satisfactory linear range and a comparable sensitivity to those of other reported colorimetric methods. However, the detection limit of the sensor designed in this study was higher than that of fluorescence and electrochemical methods for the detection of isoniazid (Table 1), which may be attributed to the different principles of isoniazid detection. On the other hand, compared to the synthesis time required for the detection of isoniazid by other nanomaterials (Table 1), the copper carbonate analog prepared in this study only requires 1.0 min for immediate isoniazid analysis. This greatly improves the efficiency of isoniazid analysis, and the synthesis process does not require high temperature, high pressure, or organic solvents. Thus, this method is suitable for the rapid preliminary detection of high concentrations of isoniazid in practical applications. Finally, to validate the selectivity of the isoniazid colorimetric platform based on the peroxidase-like activity of copper carbonate analog, the potential interferents that may be present in serum samples were added to the reaction solutions and analyzed: Cl^-, Na^+, urea, α-amylase, L-glutamic acid, L-serine, trypsin, and bovine albumin. Fig. S5 shows that the relative activity (%) is significantly affected by the presence of isoniazid. These results demonstrate that the colorimetric detection has good specificity for isoniazid.

3.7. Real samples analysis

The practical application of the isoniazid colorimetric platform was studied by analyzing the spiked recovery of the sample in

Table 2
Recovery of standard addition of isoniazid in human serum ($n = 3$).

Sample	Added (μM)	Found ± SD (μM)	Recovery (%)[a]
Human serum	0	0	–
	29.8	28.2 ± 0.1	94.8
	59.5	58.3 ± 0.4	98.0
	119.0	125.5 ± 0.6	105.5

[a] Recovery (%)=(found concentration-original concentration)/added concentration × 100.

normal human serum. Before analysis, normal human serum was diluted 500 times using absolute ethanol and centrifuged for 1.0 min. Then, the supernatant was filtered through a 0.22 μm membrane filter (Shanghai Titan Scientific Co., Ltd., Shanghai, China). The serum samples were spiked with three different concentrations of isoniazid (29.8, 59.5, and 119.0 μM). No isoniazid was found in the serum sample. The spiked recoveries (Table 2) of isoniazid in human serum samples range from 94.8% to 105.5 %, indicating the good reliability of the proposed method in detecting isoniazid in real samples.

4. Conclusions

In conclusion, copper carbonate analog with good peroxidase-like activity was successfully fabricated for the first time *via* a simple co-precipitation of $CuSO_4$■$5H_2O$ and Na_2CO_3, which has the advantages of immediate use and avoids the tedious design or synthesis processes. In addition, the kinetics assay indicates that the copper carbonate analog has a higher affinity for H_2O_2 than that of HRP. The prepared copper carbonate analog nanozyme was used for the detection of isoniazid with a LOD as low as 8.47 μM. This colorimetric detection of isoniazid has certain advantages over existing methods; however, it is also associated with certain drawbacks: 1) Relies on large instruments and requires well-skilled operators; 2) limited in its ability to detect trace amounts of isoniazid; 3) only be used to analyze a single analyte. Thus, further investigations are necessary, such as combining this method with smartphone detection and applying it to paper-based sensors for on-site detection. In short, this study presents an economical, efficient, and sensitive bio-analytical method for the detection of isoniazid, which could be utilized in pharmaceutical analysis and clinical diagnosis.

Data availability statement

Data will be made available on request.

Ethics declarations

Review or approval by an ethics committee was not needed for this study because the normal human serum used in this study was purchased from Beijing Solarbio Science and Technology Co., Ltd., China, and it is a biological product.

CRediT authorship contribution statement

Yan Dai: Writing – original draft, Methodology, Investigation, Conceptualization. **Hao Zhang:** Writing – review & editing, Supervision, Resources, Project administration, Funding acquisition, Conceptualization.

Declaration of competing interest

The authors declare that they have no known competing financial interests or personal relationships that could have appeared to influence the work reported in this paper.

Acknowledgments

This work was sponsored by the Chongqing Postdoctoral Science Foundation, China, grant number CSTB2022NSCQ-BHX0687, the Chongqing Medical Scientific Research Project (Joint project of Chongqing Health Commission and Science and Technology Bureau), China, grant number 2023MSXM006, and the Chongqing Medical and Pharmaceutical College, China, grant number ygzrc2023102. We are grateful to Ms. Zhao-Miao Gong from Chongqing Medical and Pharmaceutical College for her help in formal analysis, methodology, and software.

Appendix A. Supplementary data

Supplementary data to this article can be found online at https://doi.org/10.1016/j.heliyon.2024.e34962.

References

[1] J.J. Guo, Y. Wang, M. Zhao, 3D flower-like ferrous(II) phosphate nanostructures as peroxidase mimetics for sensitive colorimetric detection of hydrogen peroxide and glucose at nanomolar level, Talanta 182 (2018) 230–240, https://doi.org/10.1016/j.talanta.2018.01.080.

[2] M.B. Vineh, A.A. Saboury, A.A. Poostchi, A.M. Rashidi, K. Parivar, Stability and activity improvement of horseradish peroxidase by covalent immobilization on functionalized reduced graphene oxide and biodegradation of high phenol concentration, Int. J. Biol. Macromol. 106 (2018) 1314–1322, https://doi.org/10.1016/j.ijbiomac.2017.08.133.

[3] Y.L. Xian Yu, Y.P. Chen, X.Y. Jiang, Horseradish peroxidase-mediated, iodide-catalyzed cascade reaction for plasmonic immunoassays, Anal. Chem. 87 (2015) 10688–10692, https://doi.org/10.1021/acs.analchem.5b03522.

[4] L.A. Dahili, I. Kelemen-Horvath, T. Feczko, 2,4-Dichlorophenol removal by purified horseradish peroxidase enzyme and crude extract from horseradish immobilized to nano spray dried ethyl cellulose particles, Process Biochem. 50 (2015) 1835–1842, https://doi.org/10.1016/j.procbio.2015.08.008.

[5] V.G. Panferov, I.V. Safenkova, A.V. Zherdev, B.B. Dzantiev, The steadfast Au@Pt soldier: peroxide-tolerant nanozyme for signal enhancement in lateral flow immunoassay of peroxidase-containing samples, Talanta 225 (2021) 121961, https://doi.org/10.1016/j.talanta.2020.121961.

[6] L. Zhang, D. Hu, M. Salmain, B. Liedberg, S. Boujday, Direct quantification of surface coverage of antibody in IgG-Gold nanoparticles conjugates, Talanta 204 (2019) 875–881, https://doi.org/10.1016/j.talanta.2019.05.104.

[7] H. Zhang, Z.Y. Wu, Y.Y. Yang, F.Q. Yang, S.P. Li, Recent applications of immobilized biomaterials in herbal analysis, J. Chromatogr. A 1603 (2019) 216–230, https://doi.org/10.1016/j.chroma.2019.06.059.

[8] H. Wei, E.K. Wang, Nanomaterials with enzyme-like characteristics (nanozymes): next-generation artificial enzymes, Chem. Soc. Rev. 42 (2013) 6060–6093, https://doi.org/10.1039/C3CS35486E.

[9] S.R. Jin, C. Wu, Z.Z. Ye, Y.B. Ying, Designed inorganic nanomaterials for intrinsic peroxidase mimics: a review, Sensor. Actuator. B Chem. 283 (2019) 18–34, https://doi.org/10.1016/j.snb.2018.10.040.

[10] Y. Park, P.K. Gupta, V.-K. Tran, S.E. Son, W. Hur, H.B. Lee, J.Y. Park, S.N. Kim, G.H. Seong, PVP-stabilized PtRu nanozymes with peroxidase-like activity and its application for colorimetric and fluorometric glucose detection, Colloids Surf. B Biointerfaces 204 (2021) 111783, https://doi.org/10.1016/j.colsurfb.2021.111783.

[11] I. Zare, D. Choi, J. Zhang, M.T. Yaraki, A. Ghaee, S.Z. Nasab, R. Taheri-Ledari, A. Maleki, A. Rahi, K. Fan, J. Lee, Modulating the catalytic activities of nanozymes for molecular sensing, Nano Today 56 (2024) 102276, https://doi.org/10.1016/j.nantod.2024.102276.

[12] A. Jouyban, R. Amini, Layered double hydroxides as an efficient nanozyme for analytical applications, Microchem. J. 164 (2021) 105970, https://doi.org/10.1016/j.microc.2021.105970.

[13] S. Dadakhani, G. Dehghan, A. Khataee, A robust and facile label-free method for highly sensitive colorimetric detection of ascorbic acid in fresh fruits based on peroxidase-like activity of modified FeCo-LDH@WO_3 nanocomposite, Spectrochim. Acta, Part A 302 (2023) 123016, https://doi.org/10.1016/j.saa.2023.123016.

[14] S.C. Ding, J.A. Barr, Z.Y. Lyu, F.Y. Zhang, M.Y. Wang, P. Tieu, X. Li, M.H. Engelhard, Z.X. Feng, S.P. Beckman, X.Q. Pan, J.C. Li, D. Du, Y.H. Lin, Effect of phosphorus modulation in iron single-atom catalysts for peroxidase mimicking, Adv. Mater. 36 (2024) 2209633, https://doi.org/10.1002/adma.202209633.

[15] L. Yang, X.Y. Guo, Q.H. Zheng, Y. Zhang, L. Yao, Q.X. Xu, J.C. Chen, S.B. He, W. Chen, Construction of platinum nanozyme by using carboxymethylcellulose with improved laccase-like activity for phenolic compounds detection, Sensor. Actuator. B Chem. 393 (2023) 134165, https://doi.org/10.1016/j.snb.2023.134165.

[16] D.D. Yang, J.Q. Chen, Y.T. Huang, G.H. Chen, X.L. Liu, X. Wang, L.K. Yang, Z.H. Li, J. Hu, Q. Zhou, J. Ge, Y. Yang, Oxidase-like Fe–N/C single atom nanozyme enables sensitive detection of ascorbic acid and acid phosphatase, Anal. Chim. Acta 1265 (2023) 341221, https://doi.org/10.1016/j.aca.2023.341221.

[17] Y.Z. Shen, X. Gao, H.H. Chen, Y.L. Wei, H. Yang, Y. Gu, Ultrathin C_3N_4 nanosheets-based oxidase-like 2D fluorescence nanozyme for dual-mode detection of organophosphorus pesticides, J. Hazard Mater. 451 (2023) 131171, https://doi.org/10.1016/j.jhazmat.2023.131171.

[18] Y. Zhang, C.P. Wen, Y.J. Liu, A.Q. Li, Q.Y. Guo, X. Zhang, L. Fu, S. Xu, D. Qiao, P.W. Zheng, W.F. Zhu, Q.S. Pan, NIR responsive composite nanomaterials with in-situ deposition of cascaded nanozymes for multiple synergistic therapy of bacterial infection in diabetic mice, Chem. Eng. J. 470 (2023) 144345, https://doi.org/10.1016/j.cej.2023.144345.

[19] G.Y. Chen, T.Q. Chai, H. Zhang, F.Q. Yang, Applications of mild-condition synthesized metal complexes with enzyme-like activity in the colorimetric and fluorescence analysis, Coord. Chem. Rev. 508 (2024) 215761, https://doi.org/10.1016/j.ccr.2024.215761.

[20] C.Y. Zhang, H. Zhang, F.Q. Yang, Enhanced peroxidase-like activity of copper phosphate modified by hydrophilic phytic-acid and its application in colorimetric detection of hydrogen peroxide, Microchem. J. 168 (2021) 106489, https://doi.org/10.1016/j.microc.2021.106489.

[21] H. Huang, L.l. Lei, J. Bai, L. Zhang, D.H. Song, J.Q. Zhao, J.L. Li, Y.X. Li, Efficient elimination and detection of phenolic compounds in juice using laccase mimicking nanozymes, Chin. J. Chem. Eng. 29 (2021) 167–175, https://doi.org/10.1016/j.cjche.2020.04.012.

[22] S.T. Li, S.D. Zhang, Y. Tao, Y.X. Chen, Y.H. Yang, X. Liang, Q.S. Li, Construction of β-galactosidase-inorganic hybrid nanoflowers through biomimetic mineralization for lactose degradation, Biochem. Eng. J. 197 (2023) 108980, https://doi.org/10.1016/j.bej.2023.108980.

[23] F.X. Liu, D.S. Shah, G.M. Gadd, Role of protein in fungal biomineralization of copper carbonate nanoparticles, Curr. Biol. 31 (2021) 358–368, https://doi.org/10.1016/j.cub.2020.10.044.

[24] S.D. Liu, K.S. Hui, K.N. Hui, V.V. Jadhav, Q.X. Xia, J.M. Yun, Y.R. Cho, R.S. Mane, K.H. Kim, Facile synthesis of microsphere copper cobalt carbonate hydroxides electrode for asymmetric supercapacitor, Electrochim. Acta 188 (2016) 898–908, https://doi.org/10.1016/j.electacta.2015.12.018.

[25] S.P. Maputla, W.V. Dalen, A. Joubert, J. Norman, S. Castel, M. van der Merwe, L. Wiesner, A validated liquid chromatography-tandem mass spectrometry assay for the analysis of isoniazid and its metabolite acetyl-isoniazid in urine, J. Mass Spectrom. Adv. Clin. Lab 32 (2024) 11–17.

[26] N. Azizi, T. Hallaj, N. Samadi, A turn off-on fluorometric and paper-based colorimetric dual-mode sensor for isoniazid detection, Luminescence 37 (2022) 153–160, https://doi.org/10.1002/bio.4156.

[27] Y. Zhang, X. Jiang, J. Zhang, H. Zhang, Y. Li, Simultaneous voltammetric determination of acetaminophen and isoniazid using MXene modified screenprinted electrode, Biosens. Bioelectron. 130 (2019) 315–321, https://doi.org/10.1016/j.bios.2019.01.043.

[28] A.A. Lobinsky, V.P. Tolstoy, L.B. Gulina, Direct synthesis of $Co_2Al(OH)_{7-2x}(CO_3)_x{\cdot}nH_2O$ layered double hydroxide nanolayers by successive ionic layer deposition and their capacitive performance, Appl. Surf. Sci. 320 (2014) 609–613, https://doi.org/10.1016/j.apsusc.2014.09.136.

[29] L. Zhang, Q. Zhang, Q.Y. Liu, X.M. Wu, Y.M. Dong, G.L. Wang, Smart nanozyme of silver hexacyanoferrate with versatile bio-regulated activities for probing different targets, Talanta 228 (2021) 122268, https://doi.org/10.1016/j.talanta.2021.122268.

[30] W. Zhu, Y. Cheng, C. Wang, X. Lu, Fabrication of a tubular CuO/NiO biomimetic nanozyme with synergistically promoted peroxidase-like performance for isoniazid sensing, Inorg. Chem. 61 (2022) 16239–16247, https://doi.org/10.1021/acs.inorgchem.2c01896.

[31] S. Li, X.D. Zhang, Y.M. Huang, Chromium decorated leaf-like N-doped carbon anchoring with active Cr-Nx sites as oxidase mimics for isoniazid sensing, Microchem. J. 194 (2023) 109341, https://doi.org/10.1016/j.microc.2023.109341.

[32] W.Z. Yu, Q. Li, L.Q. He, R.L. Zhou, L.F. Liao, J.H. Xue, X.L. Xiao, Green synthesis of CQDs for determination of iron and isoniazid in pharmaceutical formulations, Anal. Methods 15 (2023) 944–950, https://doi.org/10.1039/D2AY01793H.

[33] L.S. Li, Y.X. Zhang, W. Gong, J. Li, Novel β-cyclodextrin doped carbon dots for host–guest recognition-assisted sensing of isoniazid and cell imaging, RSC Adv. 12 (2022) 30104–30112, https://doi.org/10.1039/D2RA05089G.

[34] R.P. Ojha, S. Pal, R. Prakash, Cu-Fe Prussian blue analog nanocube with intrinsic oxidase mimetic behaviour for the non-invasive colorimetric detection of Isoniazid in human urine, Microchem. J. 171 (2021) 106854, https://doi.org/10.1016/j.microc.2021.106854.

[35] S.B. He, L. Yang, X.L. Lin, L.M. Chen, H.P. Peng, H.H. Deng, X.H. Xia, W. Chen, Heparin-platinum nanozymes with enhanced oxidase-like activity for the colorimetric sensing of isoniazid, Talanta 211 (2020) 120707, https://doi.org/10.1016/j.talanta.2019.120707.

[36] S. Cheemalapati, S.M. Chen, M.A. Ali, F.M.A. Al-Hemaid, Enhanced electrocatalytic oxidation of isoniazid at electrochemically modified rhodium electrode for biological and pharmaceutical analysis, Colloids Surf. B Biointerfaces 121 (2014) 444–450, https://doi.org/10.1016/j.colsurfb.2014.06.035.

[37] J. Qin, L. Zhang, R. Yang, Solid pyrolysis synthesis of excitation-independent emission carbon dots and its application to isoniazid detection, J. Nano Res. 21 (2019) 59, https://doi.org/10.1007/s11051-019-4503-8.
[38] B.G. Santos, J.M. Gonçalves, D.P. Rocha, G.S. Higino, T.P. Yadav, J.J. Pedrotti, P.M. Ajayan, L. Angnes, Electrochemical sensor for isoniazid detection by using a WS_2/CNTs nanocomposite, Sens. Actuators Rep. 4 (2022) 100073, https://doi.org/10.1016/j.snr.2021.100073.
[39] W.C. Liang, H.L. Ren, Y.G. Li, H.Q. Qiu, B.C. Ye, A robust electrochemical sensing based on bimetallic metal-organic framework mediated Mo_2C for simultaneous determination of acetaminophen and isoniazid, Anal. Chim. Acta 1136 (2020) 99–105, https://doi.org/10.1016/j.aca.2020.08.044.
[40] J.J. Wang, J.H. Zhao, J. Yang, J. Cheng, Y.Z. Tan, H.H. Feng, Y.C. Li, An electrochemical sensor based on MOF-derived NiO@ZnO hollow microspheres for isoniazid determination, Microchim. Acta 187 (2020) 380, https://doi.org/10.1007/s00604-020-04305-8.